Bureau of Mines Report of Investigations/1983

Leaching Aluminum From Calcined Kaolinitic Clay With Nitric Acid

By Richard S. Olsen, William G. Gruzensky,
Sophie J. Bullard, R. P. Beyer, and Jack L. Henry

UNITED STATES DEPARTMENT OF THE INTERIOR

Leaching Aluminum From Calcined Kaolinitic Clay With Nitric Acid

By Richard S. Olsen, William G. Gruzensky,
Sophie J. Bullard, R. P. Beyer, and Jack L. Henry

CONTENTS

ILLUSTRATIONS

TABLES

UNITS OF MEASURE ABBREVIATIONS USED IN THIS REPORT

With Factors for Conversion to U.S. Customary Units

Abbreviation	Unit of measure	To convert to--	Multiply by--
atm	atmosphere	pounds per square foot	2,116
°C	degree Celsius	degree Fahrenheit	1.8 and add 32
cm	centimeter	feet	.0328
cm^2	square centimeter	square feet	.00108
cm/min	centimeter per minute	feet per minute	.0328
cm/s	centimeter per second	feet per second	.0328
cP	centipoise	pounds second per square foot	2.09×10^{-5}
cP·cm/s	centipoise centimeter per second	pounds per foot	6.85×10^{-7}
darcy	darcy	feet squared	1.062×10^{-11}
ft	foot		
g	gram	pounds	2.205×10^{-3}
g/L	gram per liter	pounds per cubic foot	.06243
h	hour		
in	inch		
in Hg	in of mercury		
L	liter	cubic feet	.03532
m	meter	feet	3.281
min	minute		
mL	milliliter	cubic feet	3.53×10^{-5}
pct	percent		
ppm	part per million		
psi	pound per square inch		
rpm	revolution per minute		
s	second		
vol pct	volume percent		
wt fr	weight fraction		
wt fr/min	weight fraction per minute		
wt pct	weight percent		

LEACHING ALUMINUM FROM CALCINED KAOLINITIC CLAY WITH NITRIC ACID

By Richard S. Olsen,[1] William G. Gruzensky,[2] Sophie J. Bullard,[3]
R. P. Beyer,[1] and Jack L. Henry[4]

ABSTRACT

Prior work by the Bureau of Mines demonstrated a feed preparation method that eliminates the formation of slime during leaching of calcined kaolinitic clay and makes leached residues fast settling and easy to filter. Nitric acid leaching rates determined for calcined kaolinitic clay prepared by this method were found to correspond to a zero-order reaction model for both batch and continuous, stirred-tank leaching. A rate constant of 0.136 min^{-1} was determined. Separation of solid residues from the reacted slurry was examined, and filtration rates were determined. Permeabilities of the flocculated, leached residues were around 51 darcys, or 5.0×10^{-7} cm^2 for laminar flow through 4-ft-deep beds.

INTRODUCTION

Kaolinitic clays offer an attractive source of aluminum because of their domestic availability, low cost, and relatively close proximity to the power sources needed in the reduction step. In the early 1960's, the Bureau of Mines prepared a series of process evaluations to compare methods of producing alumina from domestic nonbauxitic resources; the series later was updated (12).[5] In 1973 an alumina miniplant project was begun to test and develop several processes on a large scale (3). In this effort it was found that while aluminum was easily leached from calcined kaolinitic clay, it was difficult to separate the leached solids from pregnant liquors due to the small size of the residual particles. Other investigators (1, 6) have also noted and attempted to solve this problem. A feed preparation method was subsequently devised (2, 8) that allowed calcined kaolinitic clay to be leached with hydrochloric acid (HCl) in a stirred-tank reactor and then rapidly separated by either filtration or displacement washing (9). The present work reports on the leaching kinetics and liquor-residue separation of calcined clay when leached with nitric acid (HNO_3).

---

[1]Chemical engineer.
[2]Research chemist.
[3]Chemist.
[4]Supervisory research chemist.
  Albany Research Center, Bureau of Mines, Albany, OR.
[5]Underlined numbers in parentheses refer to items in the list of references at the end of this report.

FEED PREPARATION

Raw, as-mined clay was received from Thiele Kaolin Co., Sandersville, GA, in plastic bags to conserve its moisture content at 19.3 pct. The raw clay was reduced to minus 14-mesh Tyler by crushing, first in a jaw crusher to minus 1/4 in and then through three stages with a double roll crusher set at progressively closer gaps to the desired size. Sized clay was removed through a 14-mesh gyrating screen after each crushing stage, and the oversize was recrushed. The crushed clay was then wetted with a fine water mist while being tumbled on an inclined, rotating disk. Continuous feeding of crushed clay and application of about 15 g of water per kilogram of clay resulted in the particle surfaces being thoroughly wetted. Care was taken to add as much water as possible without forming agglomerations and pellets. Details of the equipment used in the feed preparation and leaching process are described in an earlier publication (9). The misted clay was dried at 275° C in an electrically heated rotary kiln with a holding time of 49 min. The dried clay was calcined at 750° C in a fluidized bed with a 34-min holding time.

BATCH LEACHING

Calcined clay was leached in a batch, stirred-tank reactor. A 5-L flask was equipped with a heating mantle and condenser to provide a boiling environment during the reaction. A low-speed paddle stirrer provided sufficient agitation to keep the clay particles in suspension. A run was made by bringing 2 L of HNO_3 of the desired strength to a boil, adding calcined clay in sufficient quantities to leave the acid in 5 pct stoichiometric excess, and allowing the reaction to proceed for a predetermined period. The time at which the acid resumed boiling after calcined clay was added was taken as time zero. The reaction was quenched after reacting for the desired time. For shorter holding times where the reaction was proceeding vigorously, 1.5 L of ice water was poured into the reactor to dilute and cool the reacting slurry. For the longer holding times it was sufficient to place the reaction flask in an ice bath where it rapidly cooled to 50° C. The products of the longer reaction times were used for conversion, settling, and filtration tests. Settling and filtration samples were pumped out of the reaction flask into 250-mL graduated cylinders. The remaining slurry was then flocculated with about 10 ppm by volume of the nonionic, high-molecular-weight, acrylamide polymer, liquid flocculant Nalco 7871[6] to make filtration easier. The residues were thoroughly washed with water to remove all process solution prior to chemical analysis.

Samples of the washed solid residues were analyzed by dissolving them in HNO_3-HF solution and determining Al and Si by atomic absorption spectrophotometry. Since essentially no silicon was leached from the calcined clay, aluminum extractions were calculated on the basis of aluminum-to-silicon ratios in the feed and residues as

$$X = \frac{(Al/Si)_f - (Al/Si)_r}{(Al/Si)_f}, \qquad (1)$$

where $(Al/Si)_f$ is the aluminum-to-silicon weight ratio in the feed and $(Al/Si)_r$ is the aluminum-to-silicon weight ratio in the residue. Use of these ratios removed any uncertainty due to water absorption gain or loss by the calcined clay or leached residue samples. It also removed the need for overall mass balances on the leaching tests.

---

[6]Reference to specific trade names does not imply endorsement by the Bureau of Mines.

TABLE 1. - Operating conditions and aluminum extraction for batch, stirred-tank leaching tests

Run	Acid	Acid conc, pct	Clay feed, g	Holding time, min	H^+ in liquor, normal	Aluminum in liquor, g/L	Fraction of aluminum extracted	Rate constant, wt fr/min
1.....	HCl	23	512	60	0.41	57.8	0.969	NAp
2.....	HNO$_3$	36	522	60	.31	59.8	.974	NAp
3.....	HNO$_3$	36	522	4.42	2.18	24.0	.543	0.123
4.....	HNO$_3$	36	522	2.68	2.95	15.8	.388	.145
5.....	HNO$_3$	50	816	60	.10	95.6	.949	NAp
6.....	HNO$_3$	45	680	60	.42	81.6	.969	NAp
7.....	HNO$_3$	45	680	4.38	2.32	35.8	.534	.122
8.....	HNO$_3$	45	680	2.38	4.24	17.2	.338	.142
9.....	HNO$_3$	40	589	60	.41	64.0	.972	NAp
10....	HNO$_3$	40	589	4.46	2.35	26.4	.556	.125
11....	HNO$_3$	40	589	2.31	3.60	15.6	.366	.159
12....	HNO$_3$	40	589	60	ND	ND	ND	NAp
13....	HCl	23	512	60	ND	ND	ND	NAp

NAp Not applicable. ND No data.

Results of the batch leaching tests are shown in table 1; note that runs 1 and 13 were made with HCl. These were done to compare the overall extractability of aluminum from the calcined clay with the two acids and to compare the effects of the two acids on settling and filtration tests. Table 1 shows that the overall extractability of aluminum was between 0.949 and 0.974 wt fr. A lower extraction was obtained in run 5, where 50-pct HNO$_3$ was used. In run 5, major difficulty was encountered with frothing and boiling over due to the concentrated solutions. Acid loss or excessive cooling to reduce frothing may account for slightly lower conversion in this test.

Reaction rate constants are shown in table 1. These were found to be independent of concentration for acid strengths between 36- and 45-pct HNO$_3$. Although it appears that the rate constants increase with holding time, this is not likely; the discrepancies are probably due to reaction rates building up as the slurry returns to its boiling temperature after clay feed is added to the reactor flask. Earlier, more comprehensive tests with HCl showed the leaching reaction to be zero order. As shown later in this report, the zero-order mechanism also correlates the results of batch and continuous leaching tests in the nitrate system.

The results of settling and filtration tests are shown in table 2. Settling tests were done in 250-mL, water-jacketed, graduated cylinders held at 50° C to ensure that Al(NO$_3$)$_3$·9H$_2$ crystals would not form in the solutions. A test was performed by adding from 1 to 20 ppm by volume of the nonionic flocculant Nalco 7871 to the slurry, mixing by inverting the graduated cylinder six times and setting it upright, and measuring the time required for the separation line between clear liquor and settling residues to pass between the graduations on the cylinder. Initial settling rates were calculated using the measured distances between the graduations. Table 2 shows that settling rates were not appreciably affected by flocculant concentration, except that if no flocculant was used the supernatant liquor remained cloudy and settling rates could not be determined. However, settling rates were strongly affected by the strength of the acid used in the leaching process. This was due to the higher density and viscosity of the more concentrated solutions. Improved settling was obtained in the fourth test of run 5 by running it at 65° C instead of 50° C, but the settling rate was still very low. Table 2 also shows the percentage of bulk solids in the slurry. Flocculated samples are shown to be less densely settled than unflocculated slurries.

TABLE 2. - Settling and filtration rates for leached clay residues from batch leaching tests

Run	Flocculant conc, ppm[1]	Settling rate, cm/min	Settled solids, vol pct	Water in cake, pct[2]	Cake depth, cm	Wash time, s	Cake permeability, darcys[3]
1.......	0	ND	26	39	2.3	56	2.6
	6	31.1	33	ND	3.2	15	13.6
	8	35.8	31	ND	2.9	14	13.2
	10	38.9	30	37	2.9	15	12.3
2.......	0	ND	18	45	2.2	23	6.1
	6	35.0	27	ND	2.6	14	11.8
	8	35.0	26	ND	2.5	18	8.9
	10	37.9	26	44	2.4	17	9.0
5.......	0	ND	34	44	4.4	303	.9
	8	.71	ND	ND	4.7	52	5.8
	10	.77	41	ND	4.6	79	3.7
	[4]10	2.32	43	46	4.5	85	3.4
6.......	0	ND	32	ND	3.8	119	2.0
	6	5.31	40	ND	4.1	19	13.8
	8	6.76	42	ND	4.0	18	14.2
	10	7.58	41	40	3.6	16	14.3
9.......	0	ND	ND	46	3.4	19	11.4
	6	16.3	38	ND	3.7	18	13.1
	8	18.2	36	ND	3.7	14	16.9
	10	21.5	36	46	3.6	22	10.4
12......	0	ND	25	47	3.3	114	1.8
	1	8.6	33	ND	3.5	41	5.4
	2	10.3	35	ND	3.6	28	8.2
	5	12.1	38	ND	3.8	24	10.1
	10	15.8	38	ND	3.9	20	12.4
	20	18.7	37	47	3.8	19	12.7
13......	0	ND	24	42	3.2	163	1.3
	1	19.9	30	ND	3.4	35	6.2
	2	23.1	29	ND	3.1	21	9.4
	5	26.4	29	ND	3.5	18	12.4
	10	27.2	35	44	2.8	17	10.5
	20	32.4	34	ND	3.6	19	12.1

ND No data.

[1]Flocculated with Nalco 7871.

[2]Bulk of water removed with vacuum before drying.

[3]In permeability tests $\mu = 1.0$ cP at $20°$ C, $V = 1,000$ mL water, $A = 19.6$ cm^2, $\Delta P = 0.80$ atm.

[4]This test done at $65°$ C instead of $50°$ C.

The slurries used in the settling tests were also used to determine the filterability or permeability of the leached residues. The graduated cylinder containing the residue to be tested was inverted and shaken gently to remix the

slurry and allow it to be poured into a modified Buchner vacuum filter. The high permeability of the residues required that the filter be relatively deep in order to contain enough wash water to provide sufficiently long filtration times. A 5-cm-diam filter funnel was extended to be 53 cm deep. A piece of 2 × 2 weave stranded twill polypropylene filter cloth supported the cake on the perforated base of the filter. After the slurry was poured into the filter, a 24-in-Hg vacuum was applied to draw off the liquor and form the filter cake. The cake was given a preliminary wash with about 500 mL of water before determining its permeability with water. This was done by adding enough water to bring the level up to a mark on the glass wall of the funnel, starting a timer, adding a measured liter of water to the funnel, and measuring the time required for the water level to return to the mark on the funnel wall. The permeability of the filter cake was defined according to D'Arcy's law as (10, pt I, p. 174)

$$K = \frac{\mu VL}{A \Delta P t}, \qquad (2)$$

where   K is permeability in darcys,

μ is viscosity in cP,

V is volume passed in cm^3,

L is cake depth in cm,

A is filter area in cm^2,

ΔP is vacuum applied in atm,

and   t is time in s.

The permeability could also be expressed in terms of length squared such as cm^2 by using the conversion factor 1 darcy is equivalent to 9.85 × 10^{-9} cm^2. The use of the darcy unit eliminates the confusion that can result when force units are

required in both the numerator and denominator of equation 2 for viscosity and pressure and the correct choice must be made.

Table 2 shows permeabilities for water at 20° C for the leached clay residues. The use of 50-pct HNO$_3$ (run 5) gave considerably lower permeability than when 45-pct HNO$_3$ was used (run 6). The last permeability test in run 5 gave the poorest results for flocculated residues; this may be due to the higher holding temperature used during settling tests, which could have caused deterioration or poorer action of the flocculant. A comparison of runs 1, 2, and 9 shows that comparable, high permeabilities were obtained when more dilute (40-pct or less) HNO$_3$ was used and that the residues of HNO$_3$ leaching are essentially the same as those obtained during HCl leaching. It should be borne in mind that the permeabilities were obtained with water and that the viscosity and density of the solutions in the original slurry did not affect these tests. Runs 12 and 13 were done to determine the level of flocculant addition required to obtain high permeabilities. These runs show that 4 to 6 ppm Nalco 7871 provides adequate flocculation for residues of either HNO$_3$ or HCl leaching.

The residues left on the filter after the permeability tests were drained for a minute or two by drawing air through the cake. Some of the cakes were weighed, dried overnight at 105° C, and reweighed to determine their water content. The fifth column in table 2 shows the moisture content of the undried cakes to be around 45 pct, which gave them the consistency of damp sand. The relatively high water content of the cake was due to the large internal porosity of the leached particles, which are silica skeletons of the original calcined clay bodies.

CONTINUOUS LEACHING

Calcined clay was leached in a continuous, three-stage, stirred-tank reactor in order to compare batch and continuous leaching behavior and to compare continuous HNO$_3$ leaching with HCl leaching tests done earlier (7, 9). The leaching

equipment consisted of three 5-L glass round-bottom flasks set up to overflow in series when they each contained 2 L of slurry. Each flask was equipped with a heating mantle to maintain boiling temperatures, a condenser to return acid and water vapors, and a low-speed paddle stirrer. The first flask was provided with means for feeding acid and calcined clay; the last reactor overflowed into a heat exchanger. The cooled slurry from the third reactor was flocculated with 10 ppm Nalco 7871 and pumped to a thickener.

The high settling rates and permeabilities found for misted clay residues allowed the use of a very small thickener and displacement washing in columns rather than the more cumbersome procedures required for more difficultly separated residues. The thickener consisted of a Y-shaped piece of 4-in-diam glass pipe. Slurry introduced to one arm of the Y separated into thickened slurry in the base of the Y and clear liquor leaving from the second arm. Thickened slurry was removed to 4-ft washing columns where the residual liquor was displaced with water. Displacement washing allowed efficient water use and minimized dilution of the pregnant liquors. Displacement washing in the columns also provided a comparison with the permeability results obtained in the earlier shallow-bed,

Buchner funnel tests on the batch-leached residues. As will be shown, the shallow-bed test led to significant underestimation of the residue permeability. Equipment used for the continuous leaching, separation, and residue washing tests was described in a previous report (9).

Two runs were made with the continuous leaching equipment, the first with a 10-min holding time per tank, or 30 min overall, and the second with 5-min per tank and 15 min overall. Samples for the 30- and 15-min tests were taken after 4.6 h and 2.7 h respectively to ensure steady state operation. The samples were pumped directly from the reaction flasks onto vacuum filter funnels to immediately separate the solids from the liquor. The last tank was sampled first, then the middle tank, then the first, so that sampling would not upset the other upstream tanks. The solid residues were washed with large quantities of water to remove any residual solution. Residue and liquor samples were sent for chemical analysis, the results of which are shown in table 3. As expected, the aluminum extracted from the calcined clay becomes greater from stage to stage, and the liquor becomes more concentrated in aluminum. The aluminum extractions shown in table 3 are plotted in figure 1 as functions of holding time.

TABLE 3. - Operating conditions and aluminum extraction
for continuous, stirred-tank leaching tests in a
three-stage reactor

Run	Holding time per stage, min	Reactor stage	H^+ in liquor, normal	Al in liquor, g/L	Fraction of aluminum extracted
C-1.....	10	1	2.99	44.8	0.668
		2	1.75	55.8	.871
		3	1.19	61.8	.937
		$(^2)$	.94	58.5	.934
C-2.....	5	1	4.01	33.5	.497
		2	2.71	49.4	.771
		3	1.75	50.8	.817
		$(^2)$	1.57	56.1	.858

[1]Liquor maintained at boiling in all stages; 40 pct HNO_3 used in both runs.
[2]Thickener underflow.

TABLE 4. - Washing rate for liquor removal from residues of run C-2

Column	Bed depth, cm	Pressure		Time to pass rinse water, s			Permeability, darcys[2]
		Gage, psi	Total, atm[1]	1st liter	2d liter	3d liter	
1.....	123	5	0.46	437	202	ND	52
2.....	125	15	1.14	185	100	105	43
3.....	125	15	1.14	160	104	93	46
4.....	129	10	.80	277	125	110	58
5.....	119	10	.79	267	122	110	54

[1]Weight of water in columns added to gage pressure.
[2]In permeability tests μ = 0.8007 cP at 30° C, A = 20.3 cm^2.

Washing data and the permeabilities of the nominally 4-ft columns are shown in table 4. Previous work (9) with the chloride system showed that the aluminum salts were readily washed from the residue and that the concentration profile was dependent on the amount of wash water passed and not on its velocity through the column. In light of this previous work, concentration profiles were not determined. However, the effect of pressure on flow rate was determined and expressed as permeabilities as shown in table 4. As shown in the table, the times to pass 3 consecutive liters of water were measured. The time to pass the first liter was about twice that required for the second or third. This was due to the higher viscosity of the aluminum nitrate solution originally in the column.

about 2.5 L, which would leave a void volume of about 1 L if the void fraction were around 0.4. The times to pass the second and third liters are therefore about the same, since most of the aluminum nitrate was removed with the first 1-L rinse. Permeabilities were calculated in the same manner as with the shallow beds, using the smaller of the two times for the water rinse. The results show permeabilities ranging between 43 and 58 darcys, or about four times as great as those shown for the shallow-bed tests. As found in the case of the chloride leaching work, the permeabilities shown by shallow-bed filtration tests may seriously underestimate the flow rates that can be obtained in deeper beds, where bed support resistance becomes less of a factor.

DISCUSSION

KINETICS OF THE LEACHING REACTION

Comparison of the batch and continuous leaching results, shown in tables 1 and 3 respectively, demonstrates the higher extraction rates obtained in the batch process. This anomaly was rationalized by applying the batch leaching rate data to a reaction model appropriate to a series of heterogeneous, back-mix reactors.

The curves in figure 1 were not drawn to pass through the points but were derived for the cases of one, two, and three tanks in series from the kinetic data generated in the batch reaction tests made with the same feed preparation. Earlier, more detailed HCl leaching tests (7) showed the clay leaching

reaction to be zero order, as would be expected in a diffusion-controlled heterogeneous reaction (5, p. 322).
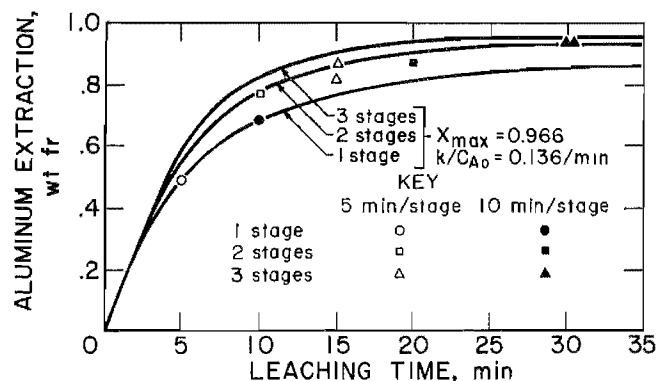

FIGURE 1. - Aluminum extraction as a function of time for continuous, cocurrent, stirred-tank reactors.

For zero-order reactions the reaction rate is independent of concentration or,

$$\frac{dC_A}{C_{AO}} = -\frac{k}{C_{AO}} dt,$$ (3)

where C_A is the concentration of component A in the clay, C_{AO} is the initial concentration, and k is a rate constant. If the reacting system were homogeneous, equation 3 would hold for all cases and particularly for both batch and continuous, stirred-tank reactors. However, in the case of clay leaching, a heterogeneous, two-phase system must be considered. Here, component A disappears from the reactor because of chemical reaction in the clay particles and also because of the loss of partially reacted particles at the reactor outlet. Loss of A by chemical reaction is governed by equation 3, which integrates to become

$$\frac{C_A}{C_{AO}} = 1 - \frac{kt}{C_{AO}}.$$ (4)

The probability (E_t) that a particle will remain in a single, ideally stirred reactor is given by

$$E_t = \left(\frac{1}{\bar{t}}\right) e^{-t/\bar{t}},$$ (5)

where t is the time considered and $\bar{t}$ is the mean residence time for the slurry in the tank. For a series of n equally sized tanks in series, the probability of a particle remaining in the reactor is

$$E_t = \left(\frac{1}{\bar{t}}\right) \frac{t}{\bar{t}}^{n-1} \frac{n^n}{(n-1)!} e^{-nt/\bar{t}},$$ (6)

where $\bar{t}$ is the mean residence time for the entire series of n equally sized tanks. If one combines equations 4 and 6, integrates between the limits 0 and C_{AO}/k (7), and makes the substitution

$$R = \frac{k\bar{t}}{C_{AO}},$$ (7)

it can be shown that overall averaged extraction ($\bar{X}$) for any number (n) of equally sized stirred tanks in series is given by

$$\bar{X}_n = R - \left[\frac{n^n}{n!} \left(\frac{1}{R}\right)^{n-1} + (R-1) \sum_{r=0}^{n-1} \frac{n^{n-1-r}}{(n-1-r)!} \left(\frac{1}{R}\right)^{n-1-r} \right] e^{-n/R}.$$ (8)

The special cases of 1, 2, 3 or an infinite number of tanks are given by

$$\bar{X}_1 = R - Re^{-1/R},$$ (9)

$$\bar{X}_2 = R - (R+1) e^{-2/R},$$ (10)

$$\bar{X}_3 = R - \left(R+2+\frac{3}{2R}\right) e^{-3/R},$$ (11)

$$\bar{X}_\infty = X_{batch} = R.$$ (12)

The above derivation assumes that all of the extractable material will be removed if the reaction is carried to completion. In fact, as shown in table 1, about 3.4

pct of the aluminum remains undissolved after 60 min and is essentially insoluble in HNO_3 or HCl. The right-hand side of the expressions in equations 8 through 12 must, therefore, be multiplied by 0.966 to compensate for the insoluble aluminum. The curves drawn in figure 1 for one, two, and three stirred tanks were constructed using a value of 0.136 min^{-1} for the rate constant k/C_{AO} and 0.966 for the maximum extractable alumina. As was found in the case of continuous HCl leaching, a correlation of the continuous, stirred-tank leaching data was provided by applying the principles of chemical reactor design to the data derived from batch, stirred-tank tests. This should allow an estimation of the size and number of tanks required in a continuous, stirred-tank HNO_3 leaching system based on preliminary, easily conducted, batch tests.

Comparison of the results of this work with the earlier investigation of the HCl leaching system (7) showed that both systems behave similarly. Both were shown to behave according to a zero-order rate model with rapid leaching of alumina from the calcined clay. The HNO_3 reaction rate was found to be about 7 pct lower than that found for HCl leaching when acids of comparable strength were used.

RATIONALIZATION OF SHALLOW-BED AND DEEP-BED PERMEABILITIES

Two objectives of this work were to compare the permeabilities of residues from HNO_3 and HCl leaching and to rationalize the differences found for permeabilities of shallow and deep beds. Permeabilities found in this work were essentially the same as those found for the HCl process (9) and showed the same dependence on bed depth.

Tables 2 and 4 show permeabilities of the leached clay residue for shallow- and deep-bed percolation tests respectively. It can be seen that even though the residues are essentially the same, the deep-bed permeabilities are about five times larger than those determined by Buchner funnel filtration tests. This wide difference was rationalized by estimating the effects of (1) the standing water column used in the Buchner funnel tests, (2) the flow resistance contributed by the filter medium bed support, and (3) the effects of turbulence on resistance to flow in the bed.

A set of flow rate tests was made using residues of continuous run C-2 in Buchner funnel tests with beds of varying depth. The conditions and results of these tests are shown in table 5. If the residues that had been washed and drained but not dried were reslurried and placed in a Buchner funnel, much lower permeabilities were obtained. However, when 10 ppm Nalco 7871 was added to the slurry, high permeabilities typical of these residues were again found.

The tests shown in table 5 were made by slurrying a quantity of residue from run C-2 in water, flocculating it with 10 ppm Nalco 7871, and pouring the slurry into the 5-cm-diam by 53-cm-deep Buchner funnel described on page 5. The walls of the funnel were glass so the water level could be seen. The desired vacuum was applied to the filter, and 1 L of water was added when the water level reached a mark on the funnel wall. The time required to pass the liter of water was measured. A series of these measurements was then made at various pressures with the same bed of leached residue. Care was taken not to allow the bed to run dry and allow air bubbles to obstruct its porosity. Tests of this type were done with beds of residue ranging between 3.7 and 19.6 cm in depth. Pressures (vacuum) ranged between 0 and 0.85 atm.

TABLE 5. – Effects of bed height and pressure drop on bed permeability

10

Column height, cm	Water temp, °C	Water viscosity, cP	Filter pressure, atm	Filter time, s	Reynolds number (Re)	$\frac{\mu V}{At}$[1], cP·cm/s	Apparent permeability, darcys	Adjusted values[2] Column height, cm	Adjusted values[2] Filter pressure, atm	Adjusted values[2] Permeability, darcys
3.7	25	0.894	0.167	39.6	13	1.15	25.5	8.2	0.220	42.9
			.334	29.4	18	1.55	17.2		.387	32.8
			.350	26.4	20	1.72	18.3		.403	35.2
			.501	23.4	22	1.95	14.4		.554	28.9
			.651	19.2	27	2.38	13.5		.704	27.7
3.8	25	.894	0	179.4	3	.25	NAp	8.3	.053	39.8
			0	174.6	3	.26	NAp		.053	40.9
			.100	58.2	9	.78	29.8		.153	42.5
			.167	43.8	12	1.04	23.7		.220	39.3
			.167	45.6	11	1.00	22.7		.220	37.7
			.334	28.2	18	1.62	18.4		.387	34.7
			.501	21.6	24	2.11	16.0		.554	31.6
			.668	18.6	28	2.45	14.0		.721	28.2
			.834	18.6	28	2.45	11.2		.887	22.9
7.0	22	.958	0	217.8	2	.22	NAp	11.5	.053	48.7
			.083	89.4	5	.55	467.1		.136	46.2
			.167	61.8	8	.79	33.1		.220	41.3
			.334	35.4	14	1.38	28.9		.387	41.0
			.334	33.0	15	1.48	31.0		.387	44.0
			.501	26.4	18	1.85	25.9		.554	38.4
			.668	22.8	21	2.14	22.5		.721	34.2
			.834	21.6	22	2.26	18.9		.887	29.3
7.6	25	.894	.100	63.0	8	.72	55.0	12.1	.153	57.0
			.167	50.4	10	.91	41.1		.220	49.8
			.350	30.0	17	1.52	33.0		.403	45.6
			.501	24.0	22	1.90	28.8		.554	41.5
			.651	21.0	25	2.17	25.4		.704	37.3
9.4	22	.958	0	286.2	2	.17	NAp	13.9	.053	44.8
			.100	88.2	5	.55	52.1		.153	50.3
			.184	60.6	8	.81	41.2		.237	47.3
			.184	58.2	8	.84	42.9		.237	49.3
			.334	39.0	12	1.25	35.3		.387	45.0
			.501	30.0	16	1.63	30.6		.554	40.9
			.668	25.8	19	1.89	26.7		.721	36.5
			.801	22.8	21	2.14	25.2		.854	34.9
19.6	23	.936	0	501.0	1	.10	NAp	24.1	.053	43.3
			.167	126.0	4	.38	44.5		.220	41.5
			.183	116.4	4	.41	43.7		.237	41.7
			.334	72.0	7	.66	38.9		.387	41.3
			.417	60.0	8	.80	37.4		.470	40.8
			.517	53.4	9	.89	33.9		.570	37.8
			.701	41.4	12	1.15	32.2		.754	36.9
			.868	36.6	14	1.30	29.5		.921	34.1

NAp Not applicable.   [1]V = 1,000 mL;   A = 19.6 cm^2.
[2]Adjusted column height includes 4.5 cm for bed support.   Adjusted pressure includes 0.053 atm for weight of water column.

The data shown in table 5 were used to estimate the effects of water head pressure and bed support losses. This was done by plotting the data as the product of viscosity and superficial velocity v of the water passed through the various columns as functions of the applied vacuum. The permeability relationship

$$K = \frac{\mu VL}{A \Delta Pt} = \frac{\mu vL}{\Delta P} \qquad (13)$$

was rearranged to express the product of viscosity and superficial velocity through the bed as a function of pressure drop and bed depth:

$$\mu v = \frac{K}{L} \Delta P. \qquad (14)$$

The pressure shown in equation 14 should be the total pressure drop across the bed, whereas the measured pressure was that of the vacuum used to pull the water through the column. The weight of the water column above the bed was accounted for by assuming an average added pressure increment P_0. The total pressure drop across the bed was then $\Delta P + P_0$, where ΔP was the gauge pressure and P_0 was that due to the water column above the bed of residue. In a similar manner, as suggested by Akers and Ward (10, pt I, pp. 169-251), resistance of the bed support can be considered as an additional bed depth L_0. Equation 14 then becomes

$$\mu v = \frac{K}{L + L_0} (\Delta P + P_0). \qquad (15)$$

The values of P_0 and L_0 were evaluated by plotting values of μv as a function of ΔP for the various column heights. These are shown in figure 2, and it can be seen that the data extrapolate to a vacuum of -0.053 atm on the abscissa. Total pressures were then computed as gauge pressure plus 0.053 atm.

Although the curves drawn in figure 2 show a distinct nonlinearity, it was assumed that this was due to the onset of turbulent flow at the higher flow

rates and that the slopes of the initial part of the curves represented the case where the flow would be laminar (nonturbulent) and equation 15 would be valid. Accordingly, the initial slopes of the curves were evaluated, and the value L_0 was calculated. It was assumed that K and L_0 were constant for all cases. The equations

$$K = a_1(L_1 - L_0) = a_2(L_2 - L_0)$$

$$= a_3(L_3 - L_0) = a_4(L_4 - L_0) \qquad (16)$$

could then be written where a_n is the slope of the initial portions of the curves and L_n is the measured bed height for the given experiment. Solution of the simultaneous equations 16 gave an average bed support resistance L_0 equivalent to 4.5 cm. Corrected bed heights were then computed by adding the 4.5 cm to the actual bed heights, as shown in table 5.

The corrected pressures and bed heights were used to calculate adjusted permeabilities. Table 5 shows that the adjusted permeabilities range from 38 to 57 darcys at low flow rates (Reynolds number less than 10) and are very similar to those obtained in the 4-ft washing columns. At higher flow rates the permeabilities decrease because of the onset of turbulent flow.
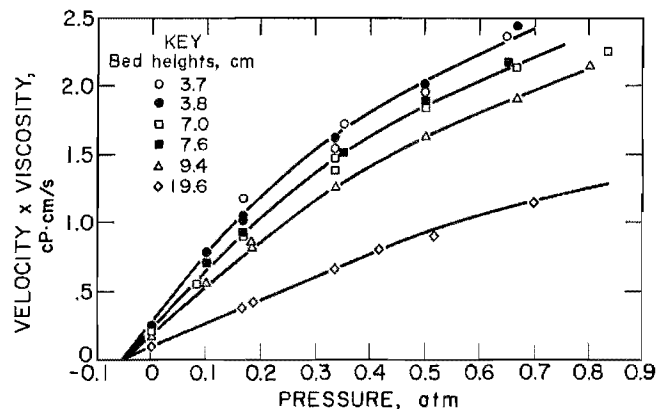

FIGURE 2. - Flow rates as functions of pressure and bed height in shallow-bed percolation tests.

The effects of turbulent flow on apparent permeabilities were estimated from packed-bed flow correlations according to Leva (4) as summarized by Perry (11, p. 5-52). In this correlation, a Fanning friction factor is defined that is inversely proportional to the Reynolds number in the case of nonturbulent flow and becomes almost constant at higher flow rates where turbulence is well developed. This correlation is directly analogous to those used to evaluate pressure drop for fluid flow in pipes and ducts, where Reynolds number (Re) is defined as

$$Re = \frac{D_p v \rho}{\mu}, \qquad (17)$$

D_p is a characteristic diameter, v is the superficial (open column) velocity, ρ is the fluid density, and μ is its viscosity. In the case of packed beds, D_p is dependent on both the size and shape of particles in the bed. Perry (11, p. 5-53) suggests relationships for estimating the effect of particle shape and size distribution on the characteristic diameter. For nonspherical particles

$$D_p = \frac{6}{\phi_s S_0} \qquad (18)$$

where ϕ_s is a shape factor and S_0 is the specific surface area of the particles.

The shape factor and specific surface can have wide ranges of values depending on the geometry of the particles involved. Assuming the residue particles resemble sand and that the sand particles can be modeled by truncated cubes having a short axis ranging between one and one-third of the longer axes, values of ϕ_s and S_0 were estimated at 0.65 and $4/d_p$, respectively. The characteristic diameter then became

$$D_p = 2.3 \, d_p. \qquad (19)$$

For residues with a size distribution the relationship

$$\frac{1}{d_p} = \Sigma \frac{x}{d_{p,x}}$$

is suggested, where x is a weight fraction and $d_{p,x}$ is the average diameter of particles in that weight fraction. The Reynolds numbers in table 5 were calculated with the above relationship using the parameters shown in table 5 and residue sizes shown in table 6.

The effect of Reynolds number on the friction factor, for flow in packed beds, is shown graphically by Perry (11, fig. 5-69, p. 5-52). For Reynolds numbers below 10, the friction factor is inversely proportional to Reynolds number, which

TABLE 6. - Wet screen analyses of feed and residues of nitric acid leaching tests

Screen size, Tyler mesh	Material, wt pct			
	Clay feed	Residue 2	Residue 6	Residue 9
Plus 20.....................	25.4	28.1	28.1	25.9
Minus 20 plus 28..........	23.2	26.2	24.4	22.3
Minus 28 plus 35..........	17.6	17.8	16.8	15.8
Minus 35 plus 65..........	12.5	11.2	11.7	12.2
Minus 48 plus 65..........	7.9	6.5	7.2	8.3
Minus 65 plus 100.........	6.5	4.9	6.5	8.4
Minus 100 plus 150........	3.9	2.8	3.0	5.6
Minus 150 plus 200........	2.4	1.8	1.8	1.6
Minus 200 plus 270........	.50	.36	.37	.40
Minus 270 plus 325........	.14	.12	.10	.15
Minus 325 plus 400........	.03	.06	.02	.02
Minus 400..................	.09	.18	.16	.13

corresponds to a constant permeability. At Reynolds numbers above 10, the friction factor decreases more slowly and deviates from the straight-line relationship shown for nonturbulent flow. If the nonturbulent straight-line relationship is extrapolated into the turbulent transition area of the graph, values of imaginary friction factors that would be expected if flow were nonturbulent can be estimated. If the values of the actual turbulent flow friction factor and the imaginary nonturbulent flow friction factor are f_T and f_L, respectively, and if the corresponding permeabilities are K_T and K_L, it can be shown that the effect of turbulence at a given Reynolds number on bed permeability should be

$$K_T = \frac{f_L}{f_T} K_L. \qquad (21)$$

A plot of permeability as a function of Reynolds number is shown in figure 3. The curve in the figure was constructed by taking the average permeability of the tests made at Reynolds numbers less than 10 to locate the straight-line portion of the curve and then estimating the effect of increasing flow rate using the correlations in Perry and equation 21 to
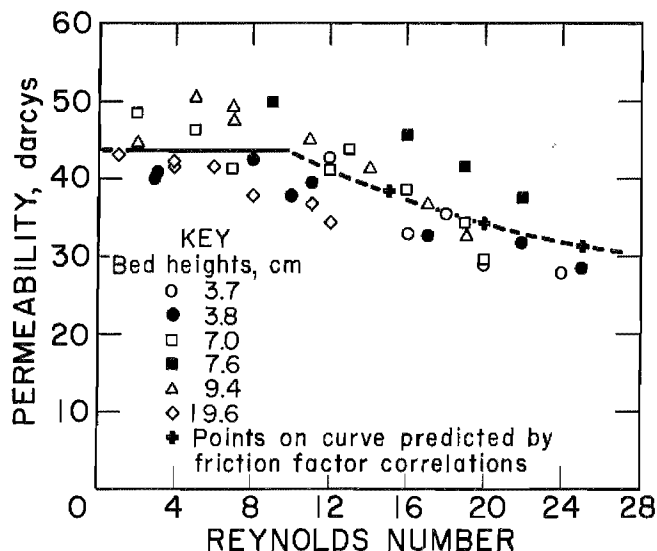

FIGURE 3. - Corrected shallow-bed permeabilities as a function of Reynolds number.

locate the dashed portion of the curve for Reynolds numbers in the turbulent transition area. For Reynolds numbers greater than 10, the curve drops off and shows the same behavior as the experimental data points. Both experimental data and theoretical considerations show that one should expect decreasing permeabilities at flows corresponding to Reynolds numbers larger than 10.

CONCLUSIONS

Batch and continuous tests showed that calcined kaolinitic clay could be easily leached when the clay was prepared by the misting process. The misting process allowed the clay to be crushed fine enough that it was easily held in suspension in a stirred-tank reactor. The misted clay was also free of very fine particles. The leached residues settled rapidly and were easily filtered.

Leaching rate data for batch and continuous stirred-tank reactors were correlated with a heterogeneous, zero-order reaction model. When the probability that a particle would or would not remain in a continuous reactor for a given time was accounted for, the zero-order model fit both batch and continuous leaching cases. The expressions derived for the

relationship between continuous single or multiple stirred-tank reactors and the batch reactor allow estimation of continuous reactor conversion from easily obtained batch reactor data. It can also be seen that the point of diminishing returns is rapidly approached and that there is little advantage in a four-tank series of reactors over a three-stage process.

Filtration data were correlated between deep- and shallow-bed tests. If shallow-bed tests are to be used to predict deep-bed washing behavior, care must be taken to account for the contribution of the filter medium to overall flow resistance. The effect of turbulence on the resistance to flow of fluids through porous media must be recognized also.

14

REFERENCES

1. Dewey, J. L., C. E. Scott, J. F. Kane, C. L. Stratton, J. C. Rushing, and R. H. Spoonts (assigned to Reynolds Metals Co.). Alumina Production by Nitric Acid Extraction of Clay. U.S. Pat. 4,246,239, Jan. 20, 1981.

2. Gruzensky, W. G. and R. S. Olsen (assigned to U.S. Dep. Interior). Extraction of Aluminum From Clay. U.S. Pat. 4,388,280, June 14, 1983.

3. Kirby, R. C., and J. A. Barclay. Alumina From Nonbauxitic Resources. Paper in Proceedings of the International Committee for the Study of Bauxite, Alumina, and Aluminum (ICSOBA-AIM Conf., Cagliari, Italy, Sept. 26-28, 1979). Academic Yugoslav der Sciences et der Arts, Zagreb, Yugoslavia, 1981, pp. 1-12.

4. Leva, M., M. Weintraub, M. Grummer, M. Pollchick, and H. H. Storch. Fluid Flow Through Packed and Fluidized Systems. BuMines B 504, 1951, 149 pp.

5. Levenspiel, O. Chemical Reaction Engineering. Wiley 1962, 501 pp.

6. Margolin, S. V., and R. W. Hyde. The ADL Nitric Acid Process for Recovery of Alumina From Aluminum-Bearing Materials. Paper in Light Metals (Proc. 103d AIME Ann. Meeting). American Institute of Mining, Metallurgical, and Petroleum Engineers, New York, v. 2, 1974, pp. 469-87.

7. Olsen, R. S., S. J. Bullard, W. G. Gruzensky, R. V. Mrazek, and J. L. Henry. Leaching Rates for the HCl Extraction of Aluminum From Calcined Kaolinitic Clay. BuMines RI 8744, 1983, 11 pp.

8. Olsen, R. S., W. G. Gruzensky, S. J. Bullard, and J. L. Henry. Effects of Feed Preparation on HCl Leaching of Calcined Kaolinitic Clay To Recover Alumina. BuMines RI 8618, 1982, 24 pp.

9. ____. Factors Affecting the Preparation of Misted Clay Feed and Solids-Liquid Separation After HCl Leaching. BuMines RI 8772, 1983, 25 pp.

10. Orr, C. Filtration Principles and Practices. Dekker 1977, pt I, 534 pp.; pt II, 407 pp.

11. Perry, R. H. Chemical Engineer's Handbook. McGraw-Hill, 5th ed., 1973.

12. Peters, F. A., and P. W. Johnson. Revised and Updated Cost Estimates for Producing Alumina From Domestic Raw Materials. BuMines IC 8648, 1974, 51 pp.